Structure of the protein kinase Cβ phospholipid-binding C2 domain complexed with Ca^{2+}

R Bryan Sutton† and Stephen R Sprang*

Background: Conventional isoforms (α, β and γ) of protein kinase C (PKC) are synergistically activated by phosphatidylserine and Ca^{2+}; both bind to C2 domains located within the PKC amino-terminal regulatory regions. C2 domains contain a bipartite or tripartite Ca^{2+}-binding site formed by opposing loops at one end of the protein. Neither the structural basis for cooperativity between phosphatidylserine and Ca^{2+}, nor the binding site for phosphatidylserine are known.

Results: The structure of the C2 domain from PKCβ complexed with Ca^{2+} and o-phospho-L-serine has been determined to 2.7 Å resolution using X-ray crystallography. The eight-stranded, Greek key β-sandwich fold of PKCβ-C2 is similar to that of the synaptotagmin I type I C2 domain. Three Ca^{2+} ions, one at a novel site, were located, each sharing common aspartate ligands. One of these ligands is donated by a dyad-related C2 molecule. A phosphoserine molecule binds to a lysine-rich cluster in C2.

Conclusions: Shared ligation among the three Ca^{2+} ions suggests that they bind cooperatively to PKCβ-C2. Cooperativity may be compromised by the accumulation of positive charge in the binding site as successive ions are bound. Model building shows that the C1 domain could provide carboxylate and carbonyl ligands for two of the three Ca^{2+} sites. Ca^{2+}-mediated interactions between the two domains could contribute to enzyme activation as well as to the creation of a positively charged phosphatidylserine-binding site.

Addresses: Howard Hughes Medical Institute and Department of Biochemistry, The University of Texas Southwestern Medical Center, 5323 Harry Hines Blvd., Dallas, TX 75235-9050, USA.

†Present address: Department of Molecular Biophysics and Biochemistry, Yale University, 266 Whitney Avenue, New Haven, CT 06520, USA.

*Corresponding author.
E-mail: sprang@howie.swmed.edu

Key words: calcium, protein conformation, protein kinases, protein structure, X-ray crystallography

Received: **13 July 1998**
Revisions requested: **18 August 1998**
Revisions received: **24 August 1998**
Accepted: **27 August 1998**

Structure 15 November 1998, **6**:1395–1405
http://biomednet.com/elecref/0969212600601395

© Current Biology Ltd ISSN 0969-2126

Introduction

Conventional (α, βI, βII and γ) isoforms of protein kinase C (PKC) are activated by diacylglycerol (DAG) and, in concert with Ca^{2+}, by acidic phospholipids, particularly phosphatidylserine (PS) [1,2]. The binding sites for these activators are located in an amino-terminal regulatory domain [3] that is composed of three functionally distinct elements. At the amino terminus is an autoinhibitory pseudo-substrate sequence which, upon activation, is thought to be released from the active site of the enzyme. The first conserved domain (C1) that follows [4] contains two cysteine-rich modules (C1A and C1B), each of which contains two potential zinc-binding sites [5]. Both modules contain a site to which DAG and phorbol esters bind, although it is the second site that plays the predominant role in phorbol-ester-induced translocation of the enzyme to the membrane [6]. The C2 domain is located at the carboxyl terminus of the PKCβ regulatory region, and is responsible for Ca^{2+}-dependent and PS-specific activation [7,8]. Although binding of either domain to its respective ligand or metal cofactor is sufficient to promote a low-affinity interaction with the plasma membrane, a high affinity interaction, which also releases the enzyme from pseudo-substrate inhibition, requires that both the C1 and C2 domains be membrane-bound (see [2] for review). DAG and phorbol esters increase the membrane affinity and PS-specificity of PKCβ [7,9]. Calcium ions also reduce the concentration of PS required for membrane binding, but have no effect on the affinity of PKCβ for phorbol esters [10,11] or phorbol-ester-induced specificity for PS over other anionic lipids [9]. Thus, the C1 and C2 domains function coordinately, although not with full synergy.

More than one hundred homologs of the C2 domain, first recognized in PKC, have been detected in a variety of membrane-associated proteins, including phospholipases, GTPase-activating proteins such as RAP and isoforms of the neurosecretory vesicle protein synaptotagmin [12,13]. C2 domains derived from synaptotagmin I (SytI) [14,15] and PKCβ [16] have been expressed as soluble recombinant proteins that bind synergistically to Ca^{2+} and acidic phospholipids, or in the case of the C2 domain of phospholipase A_2 (PLA2), to phosphatidylcholine [17]. The intrinsic affinity of the C2 domain from PKCβ for Ca^{2+} is 40–80 μM [16], similar to that reported for other C2 domains. Upon binding to PS-rich vesicles, however, the dissociation constant might fall below 1 μM, the affinity measured for PKCβ–lipid complexes [18].

The structures of four other C2 domains have been determined, including the second C2 domain from synaptotagmin I (SytI-C2A) [19] and those from PLCδ (PLCδ-C2)

[20,21], PLA_2 (PLA2-C2) [22] and PKCδ [23]. All adopt the same Greek key β-sandwich fold, which serves, in the former three proteins, as the scaffold for a bipartite Ca^{2+}-binding site that is formed by a pair of loops which project from the opposing β sheets. The C2 domains of synaptotagmin and the two phospholipases, respectively, adopt alternative type I (S-type) and type II (P-type) connectivities that differ only by circular permutation of the N and C termini with respect to the tertiary fold. As predicted by sequence analysis [12], the novel PKCs (ε, δ, η, and θ) that do not bind calcium also possess C2 domains. The C2 domain from PKCδ exhibits a type II topology similar to that of the phospholipases, although the Ca^{2+}-binding site is degenerate [23]. Conventional PKC isoforms, in contrast, are predicted to possess type I topologies, similar to that of SytI-C2A.

Only a single Ca^{2+} was located in the crystal structure of SytI-C2A, determined with crystals soaked in 100 μM Ca^{2+} [19]. Subsequent NMR and molecular-mechanics studies demonstrated that at least two Ca^{2+} can be accommodated at adjacent loci, the second with a dissociation constant of approximately 400 μM. The crystal structures of PLCδ-C2 [21,24] and PLA2-C2 [22] reveal two bound Ca^{2+}. Isothermal titration experiments indicate three Ca^{2+}-binding sites in PLCδ-C2 [25], however, and three lanthanide ions are bound in the crystal structure reported by Essen *et al.* [26]. Taken together, these structures define three adjoining Ca^{2+} subsites within a broad acidic cleft that contains the five conserved acidic residues common to all members of the C2 family that bind Ca^{2+} [13]. Each pair of adjacent Ca^{2+} ions shares a bidentate carboxylate ligand. Not all of the Ca^{2+} subsites may be occupied in any one species of C2 domain, however. Thus, using the convention of Essen *et al.* [26], SytI-C2A binds Ca^{2+} at sites II and III, whereas PLCδ-C2 and PLA2-C2 bind Ca^{2+} at sites I and II. Site II, which occupies the central position in the array, appears to have the highest affinity for Ca^{2+} and was first observed in the structure of SytI-C2A. The shared ligand field of adjacent Ca^{2+} sites suggests that Ca^{2+} binding is potentially cooperative, as has been observed in equilibrium-binding studies of PLA2-C2 [17]. Similarly, interacting Ca^{2+} sites might promote the steep, sigmoidal Ca^{2+}-dependence of phospholipid-vesicle binding observed in synaptotagmin I and PKCβ-C2 [15,16]. The structural basis of cooperativity between these two ligands is not understood, however, nor has the locus to which the phospholipids bind been discovered.

Here, we present the structure of the C2 domain of PKCβ crystallized in the presence of Ca^{2+}. The domain accommodates three Ca^{2+} ions, one of which binds at a novel site. Remarkably, one of the acidic ligands to this ion is supplied by a second C2 domain within the asymmetric unit. This, with the support of sequence analysis and model building, has prompted us to speculate that residues outside of the C2 domain, perhaps at the interface between the C1 and C2 domains, might contribute to Ca^{2+} binding. The implications of this and other structural features of PKCβ-C2 for the regulation and phospholipid specificity of PKC are discussed.

Results and discussion

Crystallization and structure determination

Alignment of homologous sequences [13] indicates that the C2 domain encompasses residues 158–280 of PKCβ. Accordingly, a GST-PKCβ-C2 fusion protein was expressed which, after thrombin cleavage, yielded a fragment encompassing residues 157–289 (15.4 kDa) of rat PKCβ preceded by 14 residues derived from the polycloning site of the pGEX-KG expression vector. This fragment (PKCβ-C2) binds Ca^{2+} with a K_d of ~60 μM and shows half-maximal cooperative binding to PS-enriched lipid vesicles [16]. PKCβ-C2 was crystallized from PEG 1500 in the presence of 2 mM $CaCl_2$. Two millimolar o-phospho-L-serine was also included as a head group analog of PS. Diffraction data were measured to a resolution of 2.7 Å resolution at ~100 K. The structure was determined by molecular replacement, using the coordinates of SytI-C2A [19] as a search model, and refined to free and conventional R factors of 0.26 and 0.22, respectively (see the Materials and method section). The asymmetric unit contains two molecules of PKCβ-C2 related by a dyad axis (Figure 1a); these are essentially identical in conformation, with a root mean square (rms) deviation of 0.16 Å between 132 pairs of equivalent Cα atoms after superposition. Molecules related by the crystallographic 2_1 axis are joined by a disulfide bond between the two Cys217 residues. Three Ca^{2+} ions are bound to each of the two molecules in the asymmetric unit. Electron density associated with one of the C2 domains in the asymmetric unit was modeled as o-phospho-L-serine and refined with partial occupancy.

Overall structure

The C2 domain of PKCβ is an antiparallel β sandwich similar in structure to the first C2 domain of synaptotagmin I with which it shares 28% amino-acid sequence identity. Each of the two sheets, designated A (β strands 1, 2, 5 and 8) and B (β strands 3, 4, 6 and 7) (Figures 1b,2a), is composed of four antiparallel β strands. The Ca^{2+}-binding sites are located between the polypeptide loops that connect β2 to β3 and β6 to β7 (CBR1 and CBR3, respectively [26]). Superposition of the four Ca^{2+}-binding C2 domain structures (Figure 2b) shows that the eight β-strand core is highly conserved. Permutation of the β sheets seems to have little impact on structural conservation: after superimposing the four domains using the 79 residues that define the structural core, the RMS deviation between the equivalent Cα atoms of PKCβ-C2 and SytI-C2A, a type I C2 fold, is 0.73 Å, whereas those for PLCδ–C2 and PLA2-C2, both type II folds, are 1.03 Å and 0.93 Å, respectively. Loop regions, including the

β2–β3 loop, which forms one wall of the Ca^{2+}-binding site, show considerable diversity in structure. In contrast, the β6–β7 loop, which forms the opposite wall of the Ca^{2+}-binding groove is relatively well conserved, although PLA2-C2 contains a one-residue deletion with respect to the other three C2 domains. Structure and sequence variation among C2 domains is most notable in the connecting loops at the end of the β sheet opposite the Ca^{2+}-binding site (Figure 2b). For example, the β7–β8 loop shows considerable structural variation.

The B sheets of C2 domains are distinctly concave. In PKCβ-C2, the curvature of this sheet is accentuated by the conformation of the β3–β4 ribbon that, in turn, might be induced by the *cis*Pro–Asp–*trans*Pro sequence beginning at position 202. The β3–β4 turn is warped against the sheet, creating a cup-like surface (Figures 1b,2a). High thermal parameters indicate that this loop is flexible. Many C2 domains possess a polybasic region formed by the hairpin loop preceding the β4 strand [13,19]. Although PKCβ-C2 contains only three basic residues in this strand, the surface of the β sheet is populated by ten positively charged residues (Figure 2a). Of these, a cluster of electrostatically uncompensated lysine residues in the β3 and β4 strands at positions 199, 197, 209, 211, and 213 endow the concave surface of sheet B with positive charge. The polybasic region in synaptotagmin I, which includes four consecutive lysine residues in the β3–β4 loop, has been implicated in protein–protein or protein–membrane interactions associated with synaptic vesicle docking or trafficking [27]. It seems unlikely, however, that the positively charged surface of sheet B in PKCβ-C2 has a similar role in phospholipid binding, as substitution of four lysine residues in this cluster with neutral residues does not inhibit association of PKCβ with PS-enriched vesicles [28]. Nevertheless, weak electron density, which we have modeled and refined as a molecule of o-phospho-L-serine at partial occupancy, is located at this site such that the phosphate group is in contact with lysines 197, 198 and 211. The absence of strong density for, and specific protein contacts with the putative seryl group suggests that the interaction might be nonspecific.

Three contiguous strands, including β3 and the β4–β5 hairpin, have been identified as the receptor for activated C kinase-1 (RACK1) binding site [29], a protein with sequence identity to heterotrimeric G protein βγ subunits that is implicated in the intracellular translocation of certain PKC isoforms [30]. These three strands form a contiguous surface of PKCβ-C2 that borders the β2–β3 ('CBR1') loop of the Ca^{2+}-binding site. Peptides derived from these sequences block translocation of activated PKCβ, suggesting that they are not accessible in the inactive enzyme.

The PKCβ-C2 domain contains a two-tiered cluster of three β bulges that span the A sheet β1, β2 and β5 strands (Figure 3). This unusual structural feature, first discovered

Figure 1

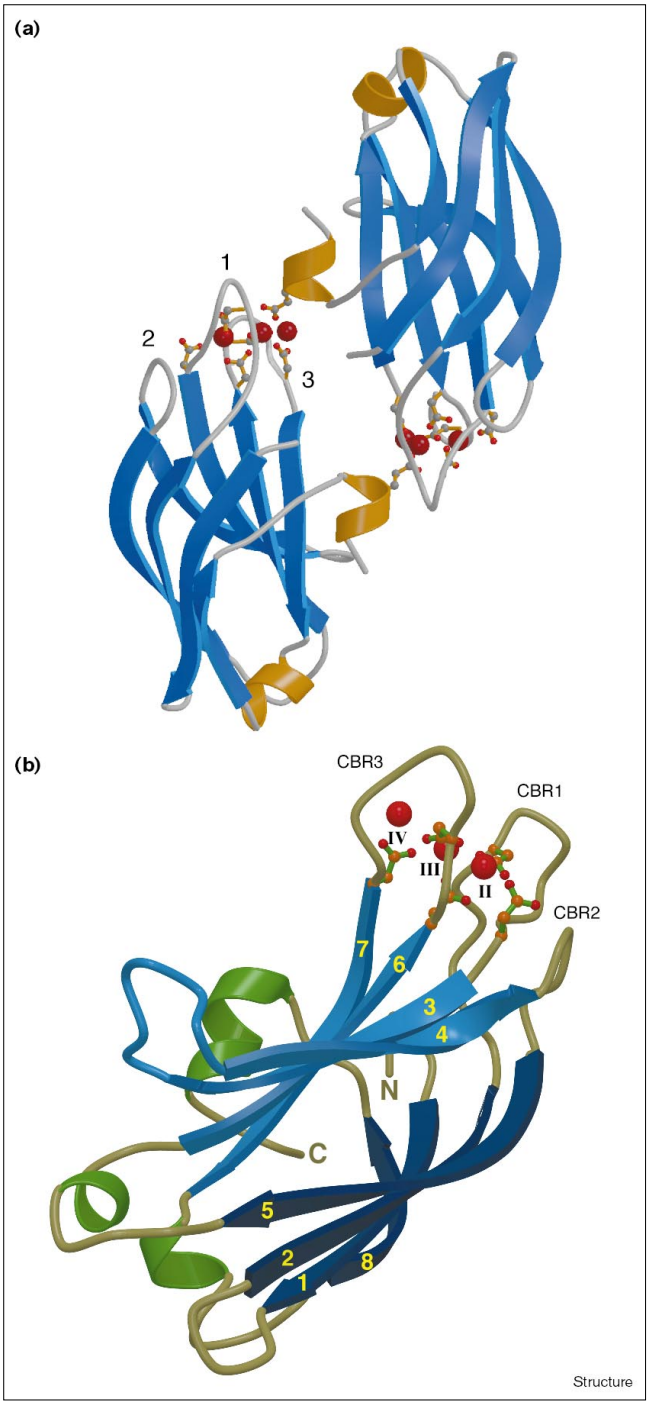

Schematic diagram of the structure of PKCβ-C2. **(a)** A ribbon model of the two C2 molecules of the asymmetric unit. β Strands are in slate blue, α helices in gold and calcium ions in red. Sidechain atoms of the five conserved acidic residues involved in calcium ligation (aspartate residues 187, 193, 246, 248 and 254) together with the intermolecular Ca^{2+} ligand, Glu281, are shown as ball-and-stick figures. Ca^{2+}-binding loops (CBR) are numbered. **(b)** A single C2 domain is shown with Ca^{2+} sites designated in Roman numerals and CBR loops numbered. β Strands are numbered with strands of sheet A in royal blue and sheet B in azure.

Figure 2

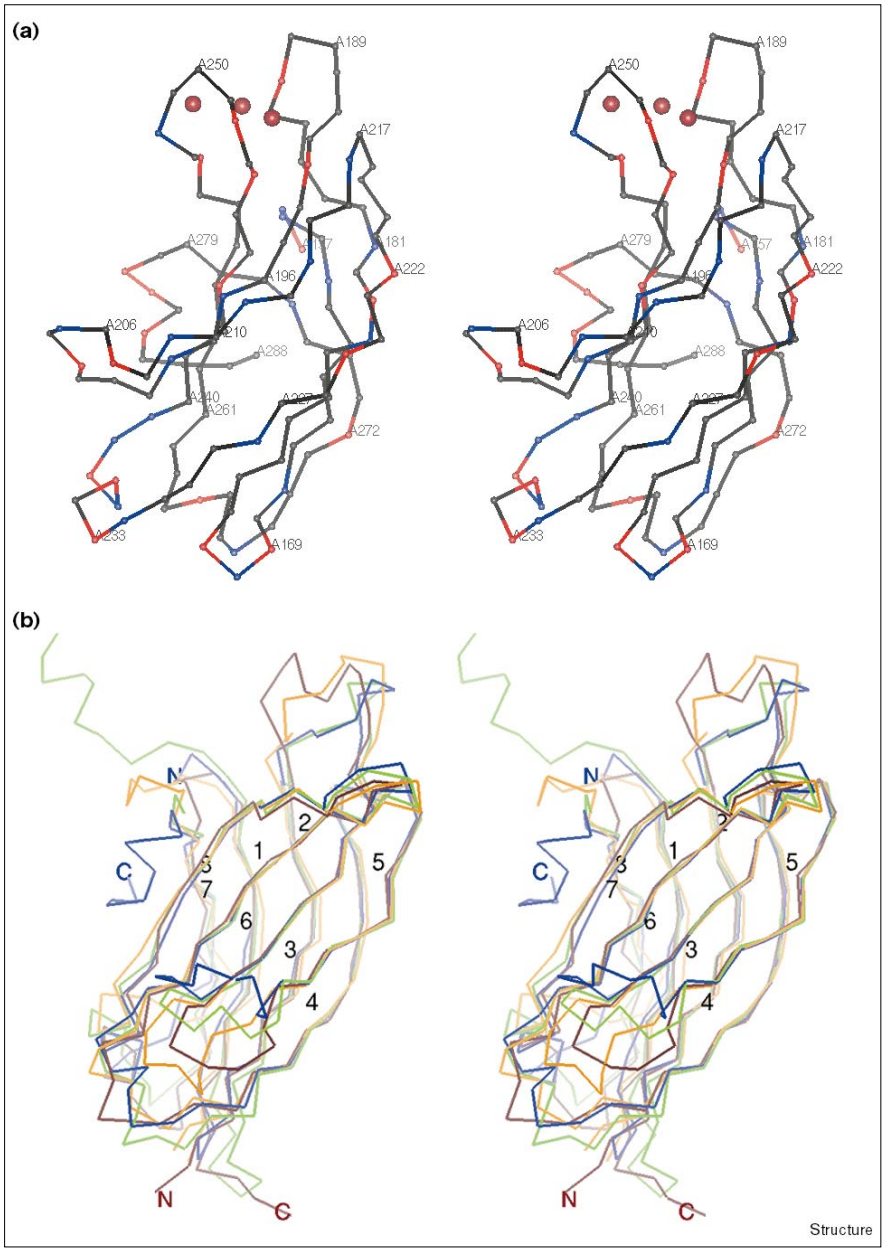

(a) Stereoview of a backbone trace of PKCβ-C2, with acidic residues (aspartate, glutamate) colored red and basic residues (histidine, lysine, arginine) in blue. **(b)** Stereoview of the PKCβ-C2 Cα backbone trace (blue), superimposed onto the C2 domains of SytI (PDB code 1RSY, green), PLCδ (1DJI, orange) and PLA2 (1RLW, burgundy) using the 79 residues (in PKCβ, residues 160–168, 172–184, 191–200, 210–219, 220–230, 240–249, 253–263 and 271–275) that constitute the β-sheet core of the C2 domain (see text).

in SytI-C2, is also conserved in the type II C2 domains of PLCδ and PLA2, as well as in the C2 domain from the novel PKCδ [23], and is therefore independent of C2-sheet topology. One of the three bulges (found in β5), in which the Arg178 carbonyl oxygen in β2 accepts hydrogen bonds from the amide groups of Trp223 and Asn224 in β5 belongs to a novel class of β bulges that has so far been observed only in C2 domains [31]. Because residues 178, 223 and 224 adopt right-, right- and left-handed helical conformations, respectively, we refer to bulges of this type as α-β bulges. Together, the three bulges impose an arch-like bend upon the three participating β strands in the plane of the sheet. The global effect of this distortion is apparently to position the β2–β3 loop relative to the opposing β6–β7 loop such that the two halves of the Ca^{2+}-binding site are correctly juxtaposed (Figure 3). C2 domains also contain a classic (+) β bulge [32,33] at the amino terminus of the β6–β7 loop. In PKCβ-C2, this structure is created by the Ile244 carbonyl oxygen, which accepts hydrogen bonds from the amide groups of Gly257 and Met256. The bend induced by this β bulge also appears to orient the β6–β7 loop of the Ca^{2+}-binding site. β Bulges therefore seem to generate the conformational distortions of the A and B sheets required to form the Ca^{2+}-binding groove. It is noteworthy that

corresponding β bulges are present in PKCδ C2 even though it does not bind Ca^{2+} [23].

At the carboxyl terminus of PKCβ-C2 is an α helix that is perpendicular to the axis of the β sandwich (Figures 1b,2a). This α helix falls outside of the C2 homology region and corresponds to part of the linker between the regulatory and catalytic domains.

Ca^{2+}-binding pocket

In aggregate, structures of C2 domain–Ca^{2+} complexes reveal three Ca^{2+}-binding subsites that are arranged linearly within a broad trough lined by aspartate residues in loops β2–β3 and β6–β7 (β1–β2 and β5–β6 in the circularly permuted PLCδ and PLA2 C2 domains). These have been defined as Ca^{2+}-binding regions (CBR) 1 and 3, respectively, by Essen *et al.* [26] (Figure 4a). The PKCβ-C2 complex contains three Ca^{2+} ions, two of which bind at loci corresponding to sites II and III (as defined by Essen *et al.* [26]) in the C2 domains of SytI-C2A and PLCδ-C2A. [16,19,26]. The third Ca^{2+} binds at a novel site within the binding cleft that we designate site IV. There is also NMR spectroscopic evidence that this site is occupied at high Ca^{2+} concentrations in the solution structure of SytI-C2 [34]. The centrally located sites II and III of PKCβ-C2 and SytI-C2 domains are related by pseudo-dyad symmetry of remarkable fidelity. The outer sites, I (occupied in PLCδ-C2) and IV, are also related by dyad symmetry, but, in contrast to II and III, their protein ligands are not. Each of the four sites shares at least one aspartate ligand with its neighbor. All three sites in PKCβ-C2 appear hexacoordinate or heptacoordinate, with Ca^{2+}-ligand coordination distances ranging from 2.4–2.6 Å. (Figure 4b). Nonprotein oxygen ligands are presumably provided by water, although none are observed in the crystal structure. The average coordination distance of 2.5 Å is only slightly larger that the Ca^{2+}–oxygen distances observed in EF-hand proteins such as calmodulin that have a higher (K_d ~10^{-5} M–10^{-7} M) affinity for Ca^{2+} [35]. These differences, however systematic, are nevertheless well within the range of coordinate error for this structure. The pseudo-dyad axis of PKCβ-C2 passes through Asp246, which contributes one carboxylate oxygen each to the Ca^{2+} bound at sites II and III. Aspartates 187 and 248 are pseudo-dyad related and both are bidentate ligands: Asp187 to Ca^{2+} II and Asp248 to Ca^{2+} III. Aspartates 187 and 248 are also monovalent ligands of Ca^{2+} III and Ca^{2+} II, respectively. The carbonyl oxygen of Trp247 coordinates the Ca^{2+} at site II, and the pseudo-symmetrically related carbonyl oxygen of Met186 ligates Ca^{2+} at site III. The fourth pair in this series of site II and III ligands are, respectively, the pseudo-dyad-related carboxylate oxygens of Asp193 and Asp254. The five aspartyl residues that contribute to site II and III Ca^{2+} coordination are conserved in the primary structures of all C2 domains that bind to Ca^{2+} [13].

Figure 3

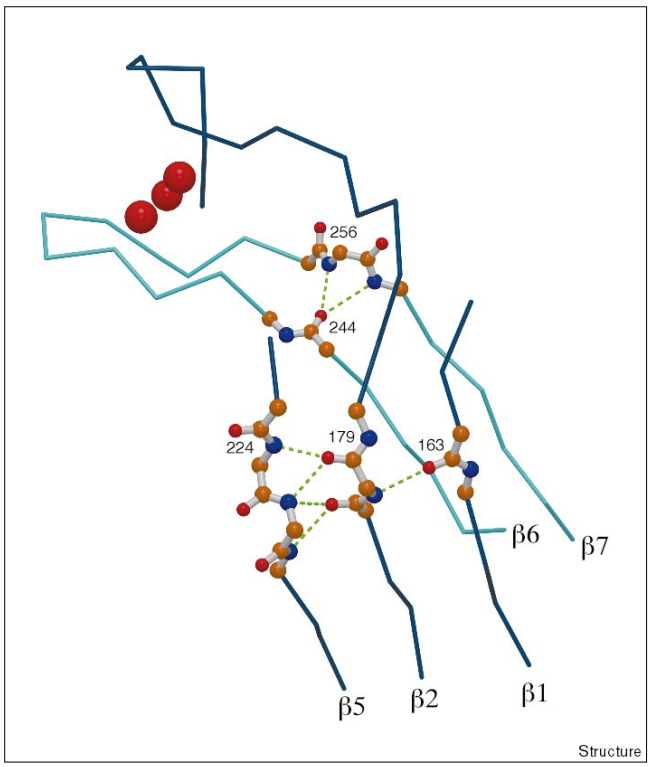

Conserved β bulges in PKCβ-C2. Water molecules are shown as large red spheres and hydrogen bonds as green dashed lines.

Ligands to the Ca^{2+} ion at site IV include Asp254 and Asp248, both of which also contribute to site III coordination, as do Ser251 and the carbonyl oxygen of Phe252. A fifth oxygen ligand is provided by Glu281 from the second C2 molecule in the asymmetric unit of the crystal. The second carboxylate oxygen of the same sidechain serves as fifth ligand to the Ca^{2+} at site III. The two molecules of the asymmetric unit are related by a pseudo-twofold axis of symmetry, but form few contacts with each other beyond the Ca^{2+} site (Figure 1a). We do not therefore impute any particular functional significance to this dimeric arrangement. The Ca^{2+}-induced dimerization of synaptotagmin I C2B domains [36] could occur by such a mechanism, however.

In crystals of SytI-C2A containing 100 μM Ca^{2+}, only site II is occupied (Figure 5). The ligand field for that ion is essentially identical to that of the corresponding site in PKCβ-C2, except that Asp230 (Asp246 in PKCβ-C2) contributes both carboxylate oxygens to the single Ca^{2+} bound in SytI-C2A. Further, Asp172 and Asp232 (the counterparts of Asp187 and ASP193 in PKCβ-C2) are disordered, as are the tips of CBR1 (residues 172–175) and CBR3 (residues 233–236), although they are fully ordered in the Ca^{2+} complex with PKCβ-C2. Analysis of Ca^{2+}-dependent NMR

Figure 4

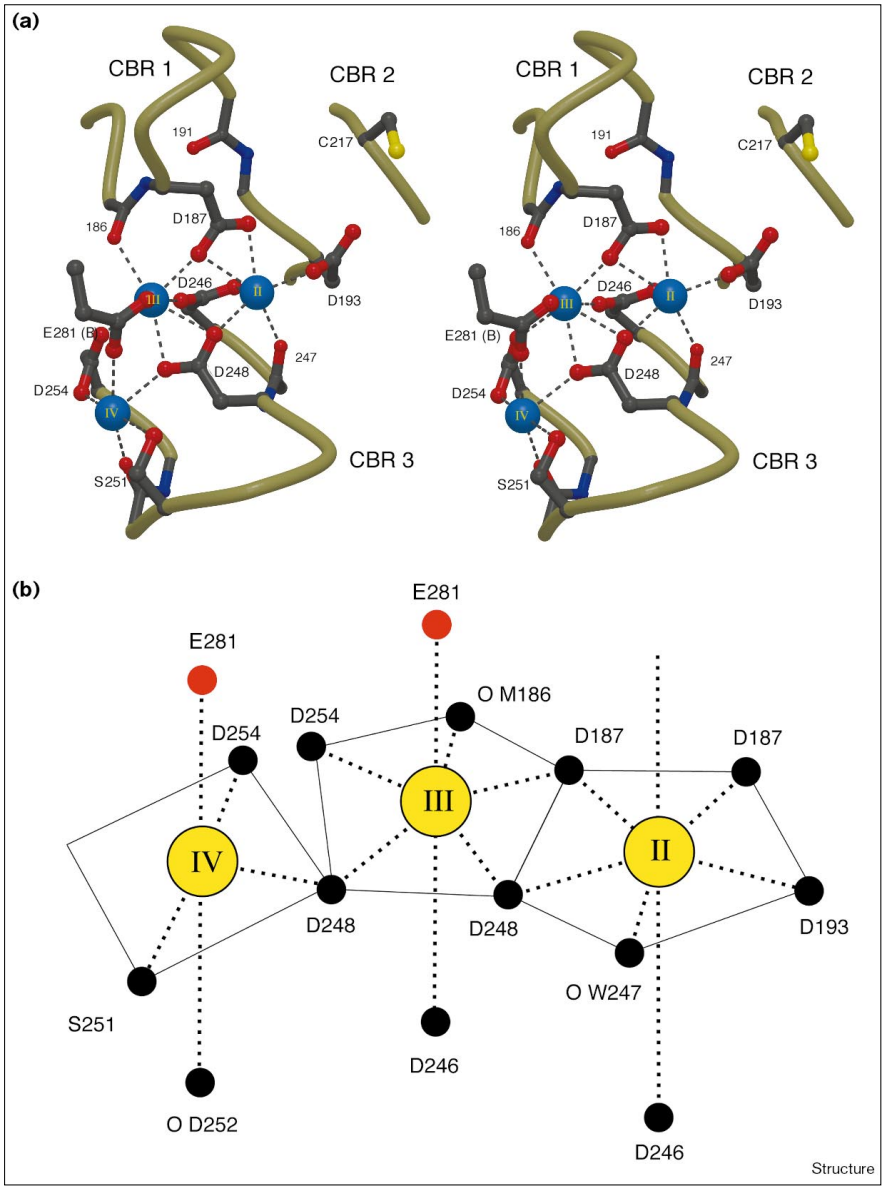

Ca^{2+}-ion ligation in C2 domains. **(a)** The Ca^{2+}-binding site of PKCβ-C2 with the polypeptide trace shown as a khaki colored tube. Mainchain and sidechain atoms involved in Ca^{2+} ligation are shown as ball-and-stick models with oxygen atoms in red, carbon atoms in charcoal and Ca^{2+} in royal blue. **(b)** Coordination of the three Ca^{2+} ions in PKCβ-C2; black spheres represent individual protein oxygen ligands. Missing ligands are shown as vertices. Oxygen atoms of Glu281, derived from the pseudo-dyad-related C2 domain (see text), are shown as red spheres. Residue labels for carbonyl oxygen ligands are preceded by 'O'. All others are sidechain carboxylate ligands.

chemical shift changes indicated that Ca^{2+} binds to site II of SytI-C2A with a K_d of approximately 60 μM. At 400 μM Ca^{2+}, site III is occupied [16]. In addition, increases in the intensity of the NOE signals indicate that these loops become more rigid as Ca^{2+} is bound, but do not change conformation. Among the C2 domains for which structures are available, SytI-C2A is the most closely related to PKCβ-C2. A comparison of the well ordered regions of the CBR1 and CBR3 loops of Ca^{2+}-free SytI-C2A with corresponding segments of PKCβ-C2 reveals no substantial differences between the two structures. Hence, by analogy to SytI-C2A, it is likely that, upon binding to PKCβ-C2, Ca^{2+} imposes rigidity upon the CBR loops, but does not induce a transition between discrete conformational states. Not considered in this analysis, however, is the possibility that conformational changes accompany synergistic interactions of Ca^{2+} and phospholipid with the C2 domain.

Although the CBR3 loops of C2 domains are structurally well conserved, there is considerable variation among the structures of CBR1 loops (Figure 5). Nevertheless, differences in the Ca^{2+}-binding properties of these domains can be attributed to sequence and structural variations in both loops. Site I, occupied in both phospholipase C2 domains, is present neither in PKCβ-C2 nor SytI-C2A. CBR2, defined by the β3–β4 loop of PLCδ-C2 and PLA2-C2 (which corresponds to β4–β5 in PKCβ-C2 topology) presents an asparagine (residues 677 and 65, respectively) to coordinate

Figure 5

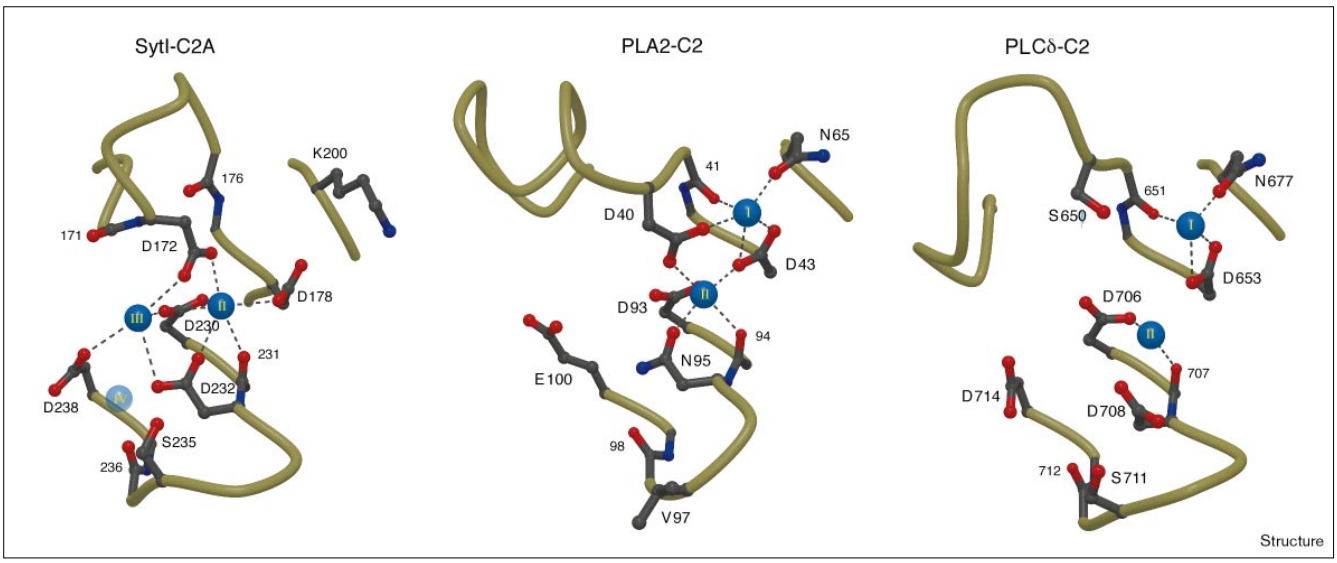

Comparison of the Ca^{2+}-binding sites of SytI-C2A, PLA2-C2 and PLCδ-C2 using the coloring scheme in Figure 4a; the weakly bound Ca^{2+} at site IV in SytI-C2A, deduced from NMR data (see text), is shown as a transparent sphere.

Ca^{2+} that is not conserved in PKCβ-C2 or SytI-C2. In crystals of PKCβ-C2, the corresponding residue, Cys217, is involved in a disulfide bridge with its symmetry mate, despite the presence of 5 mM DTT in the cryoprotectant. The CBR2 loop is only involved in site I Ca^{2+} ligation, and consequently its counterparts in PKCβ-C2 and SytI-C2 do not contribute to the Ca^{2+}-binding site. Site III is absent in PLA2-C2, due to the presence of an asparagine residue at position 95 (equivalent to Asp248 in PKCβ-C2) that is only capable of providing an oxo ligand to the Ca^{2+} bound at site II [22]. Although site II is preserved in PLCδ-C2, the analog of Asp187 in PKCβ-C2 is not its sequence equivalent Asn645, but rather the carbonyl oxygen of Ile651. The center of pseudo-symmetry that relates the calcium ligands therefore shifts to a site between Ca^{2+} I and II (Figure 5). All of the intramolecular ligands that form site IV are present in the structures of SytI-C2A and PLCδ-C2. Site IV is lost in PLA2-C2, however, due to substitution of PKCβ-C2 Ser251 by Val97 and Asp248 by Asn95.

A model for the C1–C2 domain interface

In the intact PKCβ, the C1 domain might contribute residues to Ca^{2+}-binding sites III and IV. This hypothesis is prompted by the observation that, in the crystal structure of PKCβ-C2, one of the carboxylate ligands to Ca^{2+} IV is contributed by the Glu281 of a noncrystallographic symmetry-related molecule in the crystal lattice. We propose that, in the structure of the PKCβ holoenzyme, an analogous coordinating residue is present in the carboxy-terminal C1B module of the C1 domain. The C1 and C2 domains are joined by a short linker sequence in all conventional PKC isoforms, and hence the two domains must be closely juxtaposed; perhaps intimately associated as depicted in the model of Srinivasan *et al.* [37]. In all conventional PKCs, the C1B module of the C1 domain possesses a conserved acidic residue (Asp116 in PKCβ) that is not present in most of the homologous C1A modules [38]. As shown in Figures 6a,b, the C1 and C2 domains can be juxtaposed such that Asp116, adopting a common sidechain conformation, serves as a bridging ligand of the Ca^{2+} ions bound to sites III and IV. The same orientation of the C1B domain brings Asn138 and the backbone carbonyl oxygen of the residue 139 into the coordination sphere of the Ca^{2+} in site IV. The asparagine at position 138 is also conserved in the C1B, but not the C1A domains [38]. Thus in this model, calcium ions could serve to bridge the C1 and C2 domains of PKCI. Further, in the absence of extra-domain coordination, the affinity of site IV for Ca^{2+} is likely to be weak. The juxtaposed surfaces of C1B and C2 bear negative electrostatic charge, and would not be expected to associate with high affinity (Figure 6c). In addition to coordinating acidic groups in the two domains, Ca^{2+} would tend to neutralize the electrostatic repulsion between the two domains and allow their association (Figure 6d). A similar mechanism has been invoked to explain the Ca^{2+}-dependent interaction between synaptotagmin and syntaxin [39]. Even in the absence of postulated C1–C2 domain interactions, there could be an electrostatic component to the Ca^{2+}-mediated association of phospholipids with the C2 domain, as indicated by ionic-strength dependence of the interaction [40], as well as the reduction in phospholipid affinity upon mutagenesis of arginine residues in the CBR3

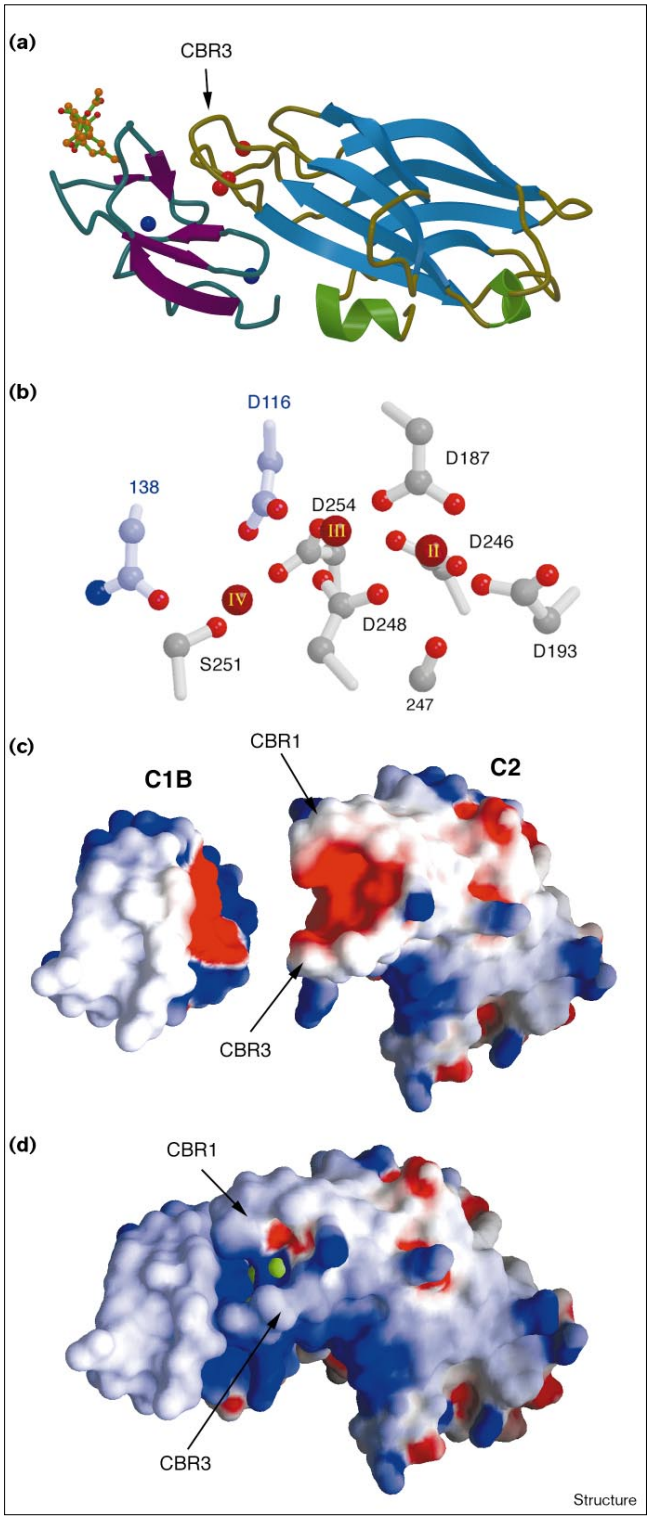

Figure 6

Models of the C1 (C1B module)–C2 domain interface of PKCβ. **(a)** A ribbon diagram colored as in Figure 1b, with the β strands of the C1B domain colored purple and loop regions in teal. Zinc atoms are colored dark blue and phorbol-13-acetate is shown as a ball-and-stick model. In the orientation shown, the upper surface of the C1B–C2 domain is proposed to contact the membrane. **(b)** Proposed Ca^{2+} ligation at the C1–C2 interface; residues derived from the C1B module are shown with lavender bonds. Oxygen atoms are colored red, nitrogen atoms blue and carbon atoms gray. **(c,d)** The molecular surface of the modeled C1B–C2 domain colored according to electrostatic potential ranging from deep blue (+10 kt/e) to red (−10 kt/e). The model is rotated about the horizontal axis by ~90°, relative to panel (a), such that the membrane-proximal surface faces the reader. The surface is shown in the absence (c) and presence (d) of Ca^{2+} (shown as green spheres with ionic radius expanded to 1.5 Å). In the absence of Ca^{2+}, electrostatic forces would be expected to disfavor association of the C1B and C2 domains, which are shown separated in (c).

loop [41]. On the other hand, charge-reversal mutations of aspartic residues in the Ca^{2+}-binding sites does not confer upon PKCβ-C2 the ability to bind phospholipids with high affinity in the absence of Ca^{2+} [28].

In the model described above, the Ca^{2+} and phorbol-ester-binding sites occupy adjacent sites on the same, presumably membrane-proximal, hydrophobic surface of the PKCβ regulatory domain. DAG and Ca^{2+}, binding respectively to the C1 and C2 domains, therefore promote association of contiguous surfaces of the regulatory domain with the plasma membrane, promoting a stronger interaction with the membrane than would be afforded by either domain acting independently. Mutagenic analysis suggests a prominent role for CRB3 in the C2 domain–membrane contact. Medkova and Cho [41] found that mutation of two tryptophan residues in CBR3 impairs Ca^{2+}-dependent association of PKCα with membrane vesicles, but not Ca^{2+} binding itself. One of these residues (Trp247 in PKCβ) is located at the proposed membrane-proximal edge strand of CBR3 (Figure 6a). Fluorescence-quenching studies of recombinant SytI-C2 domains show that tryptophan residues introduced at two sites on the corresponding surface of CRB3 also penetrate membrane vesicles [40]. The proposed mode of C2 domain–membrane interaction shown in Figure 6, although involving both CRB1 and CBR3, differs in orientation from that proposed for PLCδ [21] or PLA2 [22].

Sequential mechanisms for the activation of PKC by Ca^{2+} [41–43] suggest a multistep process in which membrane association is followed by gain of catalytic function. Full occupancy of all Ca^{2+} sites could result in closure of the C1–C2 domain interface and might be accompanied by a conformational change (such as domain rotation) that releases the enzyme from pseudo-substrate inhibition. Enhanced specificity for PS induced by DAG and Ca^{2+} might arise from the creation of a specific binding site for PS at the C1–C2 interface, perhaps within the Ca^{2+}-binding cavity itself.

This model is, of course, speculative. The function of the C1 residues Asp116 and Asn138 could be unrelated to Ca^{2+} binding, as they are also conserved in the C1B modules of novel (δ,ε,θ and η) PKC isoforms that do not bind calcium. The novel PKC isoforms possess type II topologies [13]

(placing the amino and carboxyl termini at the opposite end of the β-sandwich), however, and the order of the C1 and C2 modules is reversed relative to the conventional PKCs. Thus, the surfaces of the C1 and C2 domains proposed to form an interface in PKCβ would still be juxtaposed in the novel PKC isoforms, although the Ca^{2+}-bridging mechanism would not be possible. The C2 domain might interact with other regions of PKC in a Ca^{2+}-mediated activation mechanism. For example, phosphorylation of a serine residue within a hydrophobic site near the carboxy terminus of PKCβ increases the affinity of the enzyme for both Ca^{2+} and PS and reduces the K_m of the enzyme for ATP and peptide substrates [44]. The carboxy-terminal phosphoserine might therefore form part of the Ca^{2+}-binding site [44] in a role similar to, but which does not exclude, that which we propose for the C1 domain. The model presented here leads to the testable hypothesis that residues at the putative C1–C2 interface are involved in specific PS recognition, cooperative binding of Ca^{2+} and PS, and in the activation mechanism of PKC.

Biological implications

Conventional isoforms of protein kinase C (PKC) are stimulated by diacylglycerol (DAG) and, in concert with Ca^{2+}, acidic phospholipids, particularly phosphatidylserine (PS). These phospholipids are components of the intracellular membranes where PKC is active [1,2]. The binding sites for these activators are located in the amino-terminal regulatory domain [3], which is composed of three functionally distinct elements including the C1 and C2 domains. The C2 domain binds to Ca^{2+} and PS, whereas the C1 domain binds to DAG and phorbol esters and mediates its association with the membrane. Although PKC binds weakly to membranes in the absence of DAG and Ca^{2+}, these two activators profoundly enhance the strength of this association. Activation of PKCβ appears to proceed by a sequential mechanism with respect to Ca^{2+}, such that the concentration of Ca^{2+} sufficient to promote membrane association is less than that required to confer full enzymatic activity [42].

We show here that the C2 domain of PKC accommodates at least three Ca^{2+} ions. The three Ca^{2+} subsites share adjacent carboxylate ligands, suggesting that the metal ions can bind cooperatively, as has been demonstrated for the C2 domain of PLCδ [17]. Alternatively, the negative electrostatic potential of the binding site might be effectively neutralized after the second Ca^{2+} is bound, counteracting any cooperative, entropic effects that might confer additional binding energy. Electrostatic compensation might also underlie the heterotropic cooperativity in the binding of Ca^{2+} and acidic phospholipids [45], which are expected to prefer a positively charged binding site. Phospholipid head group binding might involve replacement of the water molecules that coordinate the Ca^{2+} ions by phospholipid oxygens, as observed in the structure of Annexin V [46]. Although present in the crystals, however, o-phospho-L-serine does not appear to bind tightly or specifically, nor are its contacts with the protein Ca^{2+}-mediated. Thus, the PS head group might not be a sufficient determinant for strong phospholipid binding. It is possible that other domains of the protein, perhaps C1, provide additional components of the head group binding site.

We have described a model for the PKC regulatory fragment in which residues derived from the C1 domain enhance the affinity of the weakest Ca^{2+}-binding sites in the C2 domain. Occupancy of all available Ca^{2+}-binding sites would lead to Ca^{2+}-mediated association of the two domains. In turn, domain association could enhance the interaction of PKC with membrane phospholipids, particularly PS, and trigger a conformational change — for example, release from pseudo-substrate inhibition — that leads to PKC activation.

Materials and methods

Purification and crystallization of PKCβ-C2

Construction of the pGEX-KG expression plasmid encoding residues 157–289 of PKCβ fused, at its amino terminus, with glutathione S transferase (GST), has been described previously [16]. *E. coli* strain BL21-DE3 cells transformed by this plasmid were grown in a BioFlo 3000 fermentor using ECPM1 media at 37°C [47]. Protein expression was induced with 100 μM IPTG followed by incubation of the cells for 3 h at 25°C. The recombinant GST-fusion protein was isolated on GST-sepharose resin [48] and after washing with phosphate buffered saline (PBS), eluted with PBS buffer containing 15 mM glutathione and 10 mM DTT. The protein was digested with thrombin (1/20 molar ratio with GST-PKCβ-C2) after dialysis against storage buffer (50 mM Tris, pH 8.5, 200 mM NaCl, 2 mM $CaCl_2$) overnight at 4°C. GST was separated from PKCβ-C2 by two rounds of gel filtration on a Superdex 200 16/10 column (Pharmacia) in storage buffer. PKCβ-C2 protein was concentrated to 65 mg/ml prior to crystallization. Protein concentration was quantified using the Pierce BCA kit.

Crystals of PKCβ-C2 were grown by vapor diffusion in hanging drops at 21°C. and enlarged by macroseeding. Droplets containing 5 μl of crystallization buffer (15% [w/v] PEG 1500, 2 mM $CaCl_2$, 2 mM o-phospho-L-serine, 100 mM MES, pH 6.4) were deposited on plastic cover slips and inverted over wells containing crystallization buffer. Small crystals harvested from these droplets were enlarged by macroseeding [49] into 10 μl sitting drops containing the equal proportions of protein solution and crystallization solution. PKCβ-C2 crystals belong to the tetragonal space group $P4_32_12$ with cell constants a = b = 77.80 Å, c = 140.83 Å and two molecules in the asymmetric unit.

Data collection and reduction

Radiation-sensitive PKCβ-C2 crystals were cryoprotected by soaking them for 5 min in cryoprotectant containing 30% PEG 400, 10% PEG 4000, 100 mM MES, pH 5.0, 2 mM $CaCl_2$, 2 mM o-phospho-L-serine and 5 mM DTT. Crystals were mounted in rayon loops and flash frozen in liquid propane. Data were measured from two crystals at the F1 beamline of the Cornell High Energy Synchrotron Source (CHESS) using radiation of wavelength 0.918 Å. Data were measured by the oscillation method with the crystal placed 116 mm from the surface of the CCD and mounted with c* coincident with the φ axis. Data were collected over a 50° range in φ, with $\Delta\phi = 0.50°$ /frame with 30s exposures/frame. Diffracted intensities were recorded using a Princeton 2K CCD (charged coupled device) detector. Images were corrected for detector distortions with the program CORRECT95 available from

CHESS. Diffraction intensities were indexed and integrated using the software package DENZO and reduced with SCALEPACK [50]. The refined crystal mosaisicity was 0.65° for both crystals. A total of 148,158 observations of 10,732 reflections were measured from crystal 1 with a merging R factor ($R_{merge} = \Sigma_{hi} |I(h)-I(h)_i| / \Sigma_{hi} I(h)_i$ where I(h) is the mean intensity after rejections) of 0.098. From crystal 2, 238,061 measurements were made of 11,912 reflections with a merging R factor of 0.14. The two were sets scaled together with a merging R of 0.136 to give a data set 98.5% complete to 2.7 Å with an average I/σ(I) of 13.0 for all reflections and 2.7 for the highest resolution shell.

Structure determination and refinement

The structure was determined by molecular replacement using the program AMoRe [51], as implemented in the CCP4 program package [52]. The core C2 domain (residues 140–265) of synaptotagmin (Protein Data Bank ID code 1RSY), excluding Ca^{2+} and solvent, was used as the search model. Residues not conserved between the $SytIC_2A$ domain and the PKC-β C2 domain were truncated to alanine in the search model. The third and fourth highest rotation function solutions, at 3.6 σ, and 3.3 σ, respectively, obtained with data in the 10–5 Å resolution shell, were related by the noncrystallographic dyad operator observed at $\Phi = 75°$, $\Psi = 0°$ in the self-rotation function. Translation searches conducted with 15–4.0 Å data in space groups $P4_12_12$ and $P4_32_12$ generated pairs of solutions with correlation coefficients of 21.3 and 28.6, respectively, establishing the latter as the correct space group enantiomorph. Rigid body refinement of the two solutions yielded a correlation coefficient of 47.9.

Phases were refined by solvent flattening, noncrystallographic symmetry averaging and histogram matching with σA weighting [53] by use of the program DM [54] in the CCP4 package. Asymmetric unit and protomer masks for solvent flattening and NCS averaging, respectively, were generated using the program MAMA [55]. Using the rigid-body refined model of the search model as a starting point, Program O,Version 5.10 [56] was used to fit the model of PKCβ–C2 to σ_A-weighted $2F_{obs}–F_{calc}$ electron density maps computed with DM-refined phases. During the course of model building the model was subjected to cycles of Powell minimization with 10–3.5 Å data followed by simulated annealing [57] using slow cooling protocols and torsion angle refinement [58] with 6.0–2.7 Å data. Final cycles of model refinement were carried out with the program CNS [59] using the amplitude based, maximum likelihood target function (MLF) and all reflections in the 20–2.7 Å range. Restrained, isotropic individual B-factors and a bulk solvent mask were used throughout the final rounds of refinement and model building. The solvent mask was generated automatically in CNS. Solvent B and scale factors of 25 $Å^2$ and 0.35, respectively, were used throughout refinement. Noncrystallographic restraints were applied to both molecules in the asymmetric unit with the exception of residues 161, 163–165, 169–171, 178, 202–208, 287 and 288. The NCS weighting term used throughout refinement was 200 kcal mol^{-1} $Å^{-2}$.

Water molecules were placed at sites where the magnitude of difference electron density > 3.0σ, and reasonable protein-solvent hydrogen bonding could be achieved without steric conflict. Six Ca^{2+} ions, which were clearly discerned early in model building were also included in the model. In addition, weak difference electron density was discerned near a cluster of lysine residues in one of the two protomers of the asymmetric unit. This density was assigned to a molecule of o-phospho-L-serine, which was included in the model with a refined occupancy of 0.56. The R_{free} and R_{work} ($R_{work} = \Sigma_h ||F_{obs}(h)|-|F_{calc}(h)|| / \Sigma_h |F_{obs}(h)|$; R_{free} was computed with a randomly selected 10% of the data removed from all refinement calculations) for the refined model is 0.254 and 0.222, respectively for the 12233 reflections in the 20–2.7 Å shell. The final model includes 2679 protein atoms, 16 heterogen atoms including six calcium ions and one molecule of o-phospho-L-serine, and 49 ordered water molecules. The model exhibits reasonable stereochemistry with rms deviations of 0.004–0.013 Å and 0.6°–3.6° from ideal bond distances and angles tabulated by Engh and Huber [60]. PROCHECK analysis [61] analysis shows that 78% of the residues adopt Φ and Ψ angles within the most favorable range and the reminder adopt values within the additional allowed range. The overall G value computed for the structure is 0.22.

Model building and analysis

The model of C1B-C2 domain was constructed manually in Program O, version 5.10 [56] using the coordinates of PKCβ-C2 and the C1B domain from protein kinase Cδ complexed with phorbol-13-acetate [62] (Protein Data Bank code 1PTR). The model was subjected to Powell minimization of potential energy terms using the program CNS [59]. Electrostatic potential calculations were carried out using the program GRASP [63] with default parameters and using the full charge set. Figure 2 was prepared using INSIGHT software (Molecular Simulations) and the remainder, excluding Figure 4b were prepared using BOBSCRIPT [64] invoked in the GL_RENDER environment by L Esser (personal communication) and rendered with RASTER-3D [65].

Accession numbers

Coordinates have been deposited with the Brookhaven Protein Data Bank with ID code 1A25.

Acknowledgements

We thank Thomas Südhof and Bazbek Davletov for a gift of the GST-PKCβ-C2 expression vector, David Coleman, John Tesmer and the staff at the F1 beam line at CHESS for assistance with data collection and Jose Rizo for sharing data before publication. This work was supported in part by Welch Foundation grant I-1229 to SRS.

References

1. Nishizuka, Y. (1995). Protein kinase C and lipid-signaling for sustained cellular responses. *FASEB J.* **9**, 484-496.
2. Newton, A.C. (1997). Regulation of protein kinase C. *Curr. Opin. Cell Biol.* **9**, 161-167.
3. Lee, M.-H. & Bell, R.M. (1986). The lipid binding, regulatory domain of protein kinase C: a 32 kDa fragment contains calcium- and phosphatidylserine-dependent phorbol diester binding activity. *J. Biol. Chem.* **261**, 14867-14870.
4. Coussens, L., Parker, P.J., Rhee, L., Yang-Feng, T.L., Chen, E., Waterfield, M.D., Francke, U. & Ullrich, A. (1986). Multiple, distinct forms of bovine and human protein kinase C suggest diversity in cellular signaling pathways. *Science* **233**, 859-866.
5. Quest, A.F.G., Bardes, E.S.G. & Bell, R.M. (1994). A phorbol ester binding domain of protein kinase Cγ. *J. Biol. Chem.* **269**, 2961-2970.
6. Szallasi, Z., Bogi, K., Gohari, S., Biro, T., Acs, P. & Blumberg, P.M. (1996). Non-equivalent roles for the first and second zinc fingers of protein kinase Cδ. *J. Biol. Chem.* **271**, 18299-18301.
7. Orr, J.W. & Newton, A.C. (1992). Interaction of protein kinase C with phosphatidylserine. 2. Specificity and regulation. *Biochemistry* **31**, 4667-4673.
8. Luo, J.-H. & Weinstein, I.B. (1993). Calcium-dependent activation of protein kinase C. *J. Biol. Chem.* **268**, 23580-23584.
9. Newton, A.C. & Keranen, L.M. (1994). Phosphatidyl-L-serine is necessary for protein kinase C's high-affinity interaction with diacylglycerol-containing membranes. *Biochemistry* **33**, 6651-6658.
10. Bazzi, M.D. & Nelsestuen, G.L. (1990). Protein kinase C interaction with calcium: a phospholipid-dependent process. *Biochemistry* **29**, 7624-7630.
11. Mosior, M. & Newton, A.C. (1996). Calcium-independent binding to interfacial phorbol esters causes protein kinase C to associate with membranes in the absence of acidic lipids. *Biochemistry* **35**, 1612-1623.
12. Ponting, C.P. & Parker, P.J. (1996). Extending the C2 domain family: C2s in PKCs δ, ε, η, θ, phospholipases, GAPs, and perforin. *Protein Sci.* **5**, 162-166.
13. Nalefski, E.A. & Falke, J.J. (1996). The C2 domain calcium-binding motif: Structural and functional diversity. *Protein Sci.* **5**, 2375-2390.
14. Davletov, B.A. & Südhof, T.C. (1993). A single C_2 domain from synaptotagmin I is sufficient for high affinity Ca^{2+}/phospholipid binding. *J. Biol. Chem.* **268**, 26386-26390.
15. Chapman, E.R. & Jahn, R. (1994). Calcium-dependent interaction of the cytoplasmic region of synaptotagmin with membranes. *J. Biol. Chem.* **269**, 5735-5741.
16. Shao, X., Davletov, B.A., Sutton, R.B., Südhof, T.C. & Rizo, J. (1996). Bipartite Ca^{2+}-binding motif in C_2 domains of synaptotagmin and protein kinase C. *Science* **273**, 248-251.

17. Nalefski, E.A., Slazas, M.M. & Falke, J.J. (1997). Ca^{2+}-signaling cycle of a membrane-docking C2 domain. *Biochemistry* **36**, 12011-12018.
18. Mosior, M. & Epand, R.M. (1998). Characterization of the calcium-binding site that regulates association of protein kinase C with phospholipid bilayers. *J. Biol. Chem.* **269**, 13798-13805.
19. Sutton, R.B., Davletov, B.A., Berghuis, A.M., Südhof, T.C. & Sprang, S.R. (1995). Structure of the first C_2 domain of synaptotagmin I: a novel Ca^{2+}/phospholipid-binding fold. *Cell* **80**, 929-938.
20. Essen, L.-O., Perisic, O., Cheung, R., Katan, M. & Williams, R.L. (1996). Crystal structure of a mammalian phosphoinositide-specific phospholipase Cδ. *Nature* **380**, 595-602.
21. Grobler, J.A., Essen, L.-O., Williams, R.L. & Hurley, J.H. (1996). C2 Domain conformational changes in phospholipase c-δ1. *Nat. Struct. Biol.* **3**, 788-795.
22. Perisic, O., Fong, S., Lynch, D.E., Bycroft, M. & Williams, R.L. (1998). Crystal structure of a calcium-phospholipid binding domain from cytosolic phospholipase A2. *J. Biol. Chem.* **273**, 1596-1604.
23. Pappa, H., Murray-Rust, J., Dekker, L.V., Parker, P.J. & McDonald, N.Q. (1998). Crystal structure of the C2 domain from protein kinase C-δ. *Structure* **6**, 885-894.
24. Williams, R.L. & Katan, M. (1996). Structural views of phosphoinositide-specific phospholipase C: signalling the way ahead. *Structure* **4**, 1387-1394.
25. Grobler, J.A. & Jurley, J.H. (1998). Catalysis by phospholipase C δ_1 requires that Ca^{2+} bind to the catalytic domain but not the C2 domain. *Biochemistry* **37**, 3020-3028.
26. Essen, L.O., Perisic, O., Lynch, D.E., Katan, M. & Williams, R.L. (1997). A ternary metal-binding site in the C2 domain of phosphoinositide-specific phospholipase C-delta-1. *Biochemistry* **36**, 2753-2762.
27. Bommert, K., Charlton, M.P., DeBello, W.M., Chin, G.J., Betz, H. & Augustine, G.J. (1993). Inhibition of neurotransmitter release by C2-domain peptides implicates synaptotagmin in exocytosis. *Nature* **363**, 163-165.
28. Edwards, A.S. & Newton, A.C. (1997). Regulation of protein kinase C βII by its C2 domain. *Biochemistry* **36**, 15615-15623.
29. Ron, D., Luo, J. & Mochly-Rosen, D. (1995). C2 region-derived peptides inhibit translocation and function of β protein kinase C *in vitro*. *J. Biol. Chem.* **270**, 24180-24187.
30. Ron, D., Chen, C.-H., Caldwell, J., Jamieson, L., Orr, E. & Mochly-Rosen, D. (1994). Cloning of an intracellular receptor for protein kinases C: A homolog of the β subunit of G proteins. *Proc. Natl Acad. Sci. USA* **91**, 839-843.
31. Sutton, R.B. (1998). Crystal structures of three Ca^{2+}-dependent phospholipid binding proteins: annexin IV and the C2 domains of syntaptotagmin I and protein kinase Cβ1 [PhD thesis]. University of Texas Southwestern Medical Center, Dallas, Texas.
32. Richardson, J.S., Getzoff, E.D. & Richardson, D.C. (1978). The β bulge: A common small unit of nonrepetitive protein structure. *Proc. Natl Acad. Sci. USA* **75**, 2574-2578.
33. Chan, A.W.E., Hutchinson, E.G., Harris, D. & Thornton, J.M. (1993). Identification, classification, and analysis of beta-bulges in proteins. *Protein Sci.* **2**, 1574-1590.
34. Ubach, J., Zhang, X., Shao, X., Südhof, T.C. & Rizo, J. (1998). Ca^{2+} binding to synaptotagmin: How many Ca^{2+} bind to the tip of a C2-domain? *EMBO J.* **17**, 3921-3930.
35. Strynadka, N.C.J. & James, M.N.G. (1989). Crystal structures of the helix–loop–helix calcium-binding proteins. *Annu. Rev. Biochem.* **58**, 951-998.
36. Chapman, E.R., An, S., Edwardson, J.M. & Jahn, R. (1996). A novel function for the second C2 domain of synaptotagmin. *J. Biol. Chem.* **271**, 5844-5849.
37. Srinivasan, N., Bax, B., Blundell, T.L. & Parker, P.J. (1996). Structural aspects of the functional modules in human protein kinase Cα deduced from comparative analyses. *Proteins* **26**, 217-235.
38. Hurley, J.H., Newton, A.C., Parker, P.J., Blumberg, P.M. & Nishizuka, Y. (1997). Taxonomy and function of C1 protein kinase C homology domains. *Protein Sci.* **6**, 477-480.
39. Shao, X., Li, C., Fernandez, I., Zhang, X., Südhof, T.C. & Rizo, J. (1997). Synaptotagmin-syntaxin interaction: the C2 domain as a Ca^{2+}-dependent electrostatic switch. *Neuron* **18**, 133-142.
40. Chapman, E.R. & Davis, A.W. (1998). Direct Interaction of a Ca^{2+}-binding Loop of Synaptotagmin with Lipid Bilayers. *J. Biol. Chem.* **273**, 13995-14001.
41. Medkova, M. & Cho, W. (1998). Mutagenesis of the C2 Domain of Protein Kinase C-α. *J. Biol. Chem.* **273**, 17544-17552.
42. Bazzi, M.D. & Nelsestuan, G.L. (1991). Highly sequential binding of protein kinase C and related proteins to membranes. *Biochemistry* **30**, 7970-7977.
43. Keranen, L.M. & Newton, A.C. (1997). Ca^{2+} differentially regulates conventional protein kinase Cs' membrane interaction and activation. *J. Biol. Chem.* **272**, 25959-25967.
44. Edwards, A.S. & Newton, A.C. (1997). Phosphorylation at conserved carboxyl-terminal hydrophobic motif regulates the catalytic and regulatory domains of protein kinase C. *J. Biol. Chem.* **272**, 18382-18390.
45. Newton, A.C. (1995). Protein kinase C structure, function, and regulation. *J. Biol. Chem.* **270**, 28495-28498.
46. Swairjo, M.A., Concha, N.O., Kaetzel, M.A., Dedman, J.R. & Seaton, B.A. (1995). Ca^{2+}-bridging mechanism and phospholipid head group recognition in the membrane-binding protein annexin V. *Nat. Struct. Biol.* **2**, 968-974.
47. Bernard, A. & Payton, M. (1995). Fermentation and growth of *Escherichia coli*. for optimal protein production. In *Current Protocols in Science*. pp. 1-18, John Wiley & Sons, Inc., New York.
48. Smith, D.B. & Johnson, K.S. (1988). Single-step purification of polypeptides expressed in *Escherichia coli* as fusions with glutathione S-transferase. *Gene* **67**, 31-40.
49. Thaller, C., Weaver, L.H., Eichele, G., Wilson, E., Karlsson, R. & Jasonius, J.N. (1981). Repeated seeding techniques for growing large single crystals of proteins. *J. Mol. Biol.* **147**, 465-469.
50. Otwinowski, Z. (1993). Oscillation data reduction program. In *Data collection and processing. (*Sawyer, N.I.L. & Bailey, S.W., eds), pp 56-62, Science and Engineering Council Daresbury Laboratory, Daresbury, U.K.
51. Navaza, J. (1994). *AMoRe*: an automated package for molecular replacement. *Acta Crystallogr A* **50**, 157-163.
52. Collaborative computational project, No. 4. (1994). The CCP4 Suite:programs for protein crystallography. *Acta Crystallogr. D* **50**, 760-763.
53. Read, R.J. (1990). Structure-factor probabilities for related structures. *Acta Crystallogr. A* **46**, 900-912.
54. Cowtan, K.D. (1994). DM Program. *Joint CCP4-ESF-EACBM Newslett.* **31**, 34-38.
55. Kleywegt, G.J. and Jones, T.A. (1994). In *Proceedings of the CCP4 Study Weekend*. pp. 59-66, Science and Engineering Council Daresbury Laboratory, Warrington, UK.
56. Jones, T.A., Zou, J.-Y., Cowan, S.W. & Kjeldgaard, M. (1991). Improved methods for building protein models in electron density maps and the location of errors in these models. *Acta Crystallogr. A* **47**, 110-119.
57. Brünger, A.T., Krukowski, A. & Erickson, J.W. (1990). Slow-cooling protocols for crystallographic refinement by simulated annealing. *Acta Crystallogr. A* **46**, 585-593.
58. Rice, L.M. & Brünger, A.T. (1994). Torsion angle dynamics: reduced variable conformational sampling enhances crystallographic structure refinement. *Proteins* **19**, 277-290.
59. Brünger, A.T.*et al.* (1998). Crystallography and NMR system (CNS): a new software suite for macromolecular structure determination. *Acta Crystallogr.* D, in press.
60. Engh, R.A. & Huber, R. (1991). Accurate bond and angle parameters for X-ray protein structure refinement. *Acta Crystallogr. A* **47**, 392-400.
61. Laskowski, R.A., MacArthur, M.W., Moss, D.S. & Thornton, J.M. (1993). PROCHECK: a program to check the stereochemical quality of protein structures. *J. Appl. Crystallogr.* **26**, 283-291.
62. Zhang, G., Kazanietz, M.G., Blumberg, P.M. & Hurley, J.H. (1995). Crystal structure of the Cys2 activator-binding domain of protein kinase Cδ in complex with phorbol ester. *Cell* **81**, 917-924.
63. Nicholls, A., Sharp, K.A. & Honig, B. (1991). Protein folding and association: insights from the interfacial and thermodynamic properties of hydrocarbons. *Proteins* **11**, 281-296.
64. Esnouf, R. (1997). An extensively modified version of MolScript that includes greatly enhanced coloring capabilities. *J Mol. Graphics* **15**, 133-138.
65. Merritt, E.A. & Murphy, M.E.P. (1994). Raster 3D version 2.O: A program for photorealistic graphics. *Acta Crystallogr. D* **50**, 869-873.